Great Slave Lake Water Resources

Using Earth Observations to Monitor Water Quality of Great Slave Lake in the Northwest Territories, Canada

Spring 2025 | Massachusetts – Boston

April 4th, 2025

Authors: Rachel Vered (Analytical Mechanics Associates), Christopher Fan (Analytical Mechanics Associates), Declan Hogan (Analytical Mechanics Associates), Eliza Lawrence (Analytical Mechanics Associates)

Abstract: Great Slave Lake in Canada's Northwest Territories (NWT) is a vital freshwater resource that supports local fisheries and tourism. Recent increases in sediment concentrations from the Slave River affect Great Slave Lake's water quality. The Government of the NWT (GWNT) Water Research and Monitoring Section collects in situ water quality data, but due to limited resources they lack large-scale spatial and temporal insights into turbidity patterns. To address these challenges, we developed turbidity algorithms using in situ turbidity and reflectance data. We then applied these algorithms to imagery from NASA's Aqua Moderate Resolution Imaging Spectroradiometer (MODIS), European Space Agency's Ocean Colour Climate Change Initiative (OC-CCI), and Sentinel-3A Ocean Land Color Instrument to assess the feasibility of using the shorter-wavelength sensors (MODIS and OC-CCI) for turbidity monitoring over long time scales. Using OC-CCI, we constructed a time series of monthly average turbidity from June to October, 2002 to 2024 for Great Slave Lake and five sub-sections: North Finger, North Mid-Arm, Central Basin, South Basin, and East Arm. We also analyzed the seasonality of turbidity and its relationship with Slave River discharge. To validate algorithms, we compared in situ turbidity measurements to Sentinel-2 Multispectral Imager (MSI) derived values. The results suggest OC-CCI is feasible for measuring turbidity. There were no observable long-term turbidity trends in Great Slave Lake, but turbidity was highest in the North Finger and lowest in the East Arm, with noticeable spikes in 2011 and 2020. Great Slave Lake turbidity was not significantly influenced by Slave River discharge. Despite limitations, our approach offers a cost-effective, scalable solution for improving water resource management in Great Slave Lake.

Key Terms: turbidity, Ocean-Colour-CCI, reflectance, in situ, river discharge, seasonality, Slave River, subarctic

Advisor: Dr. Cédric Fichot (Boston University)
Lead: Madi Arndt (MA – Boston)

1. Introduction

1.1 Background Information

Great Slave Lake, located in Canada's Northwest Territories (NWT), is one of the world's largest freshwater lakes (Figure 1). Its drainage basin spans 380,000 square miles and extends into parts of British Columbia, Alberta and Saskatchewan (Pearson, 1970). The majority of water flows into Great Slave Lake from the Slave River from the south and out via the Mackenzie River from the west, that eventually drains into the Arctic Ocean (Evans and Muir 2016; Gibson et al., 2006).

Figure 1. Study area map of Great Slave Lake.

Great Slave Lake is an important water resource for the region and local communities. Great Slave Lake is home to 60% of the population of the NWT and supports residents economically through fisheries, tourism and transportation (Rühland et al., 2023). Tribal nations rely on Great Slave Lake for its variety of fish species, such as trout, burbot, and lake whitefish, and have operated commercial fisheries since the 1940s (Evans and Muir, 2016). Historically, the Slave River creates large sediment plumes as it empties into Great Slave Lake, impacting the lake's water quality and habitats. The discharge of the Slave River and its suspended sediment contribution vary seasonally and are affected by climate. In recent years, increased precipitation and warming trends have increased river inflow leading to increased algal blooms (Gibson et al., 2006). Thus, there is an urgent need for consistent water quality monitoring throughout Great Slave Lake to track climate change-related trends.

However, few long-term studies have examined Great Slave Lake's water quality due to the cost and logistic challenges associated with its remote location. While one previous study used MODIS satellite imagery alongside in situ data to investigate changes in surface temperature, most studies have relied solely on field observations which are time-consuming and difficult to collect (Pour, 2011). This leads to shorter study periods and limited ability to extrapolate over a large study area, highlighting the need to explore the feasibility of incorporating other collection methods. The growing availability of satellite-based optical remote sensing data has made it possible to conduct time series analyses of large freshwater systems, such as Great Slave Lake, enabling greater spatial and temporal coverage.

The optical remote sensing used in this project measured the remote-sensing reflectance of water bodies, which is directly dependent on the optical properties and concentrations of the water constituents. Turbid waters with high concentrations of suspended sediment have a much higher reflectance in the red and near-infrared regions than waters with low concentrations of suspended sediment. A study conducted by Dogliotti

et al. (2015) established a well-performing mathematical relationship between water reflectance of the near-infrared (NIR) band at 859 nm and turbidity.

1.2 Project Partners & Objectives

We partnered with the Government of the Northwest Territories Water Research and Monitoring Section (GNWT), K'atl'odeeche First Nation Land and Resources Division (KFN), and Akaitcho Territory Government Aboriginal Aquatic Resource & Oceans Management (ATG), to monitor long-term changes in Great Slave Lake's water quality using Earth observation data. Our partners currently monitor Great Slave Lake through in situ data collection as part of their community-based Water Quality Program, measuring parameters such as pH, turbidity, and chlorophyll-a (chl-a) (NWT Water Stewardship, n.d.). However, they have faced challenges in obtaining consistent monitoring data due to Great Slave Lake's size, terrain accessibility, limited funding and resources, and permitting regulations. As they aim to make informed decisions on water resource management, they require reliable and consistent data to access long-term trends.

This feasibility study addressed these challenges by using Earth observations to quantify changes in Great Slave Lake's turbidity over time. Our partners have monitored water quality since 2012 which provided a reference to compare our Earth observations to in situ data (Government of the Northwest Territories, n.d.). We chose a study period from 2002 to 2024 to ensure sufficient overlap for comparison and based it on the availability of imagery with appropriate spatial resolution. Including years before in situ monitoring allowed us to better analyze historical trends that can benefit our partner's monitoring efforts. We utilized OC-CCI and Sentinel-3 data, to produce maps and time series visualizations of turbidity trends, focusing on annual and seasonal patterns. To provide greater insight into determinants and trends for turbidity, we split up the analysis of our study area into two categories: regional and localized (Figure 2). For the regional extents, we analyzed turbidity for all Great Slave Lake and then split up the lake into smaller sections that we named: North Finger, North Mid-Arm, Central Basin, South Basin, and East Arm. We also performed a localized analysis of turbidity at a finer spatial resolution around three primary population centers, Hay River, Fort Resolution, and Yellowknife, to demonstrate the capacity of remote sensing to provide detailed turbidity mapping. These results will help inform the NWT's Water Stewardship Strategy and can be applied to regional planning, emergency response, and resource management. The results of this project demonstrate how Earth observations can be used to enhance local water quality monitoring techniques and enable communities to make water resource management decisions guiding local fisheries and recreation in accordance with fluctuating turbidity levels.

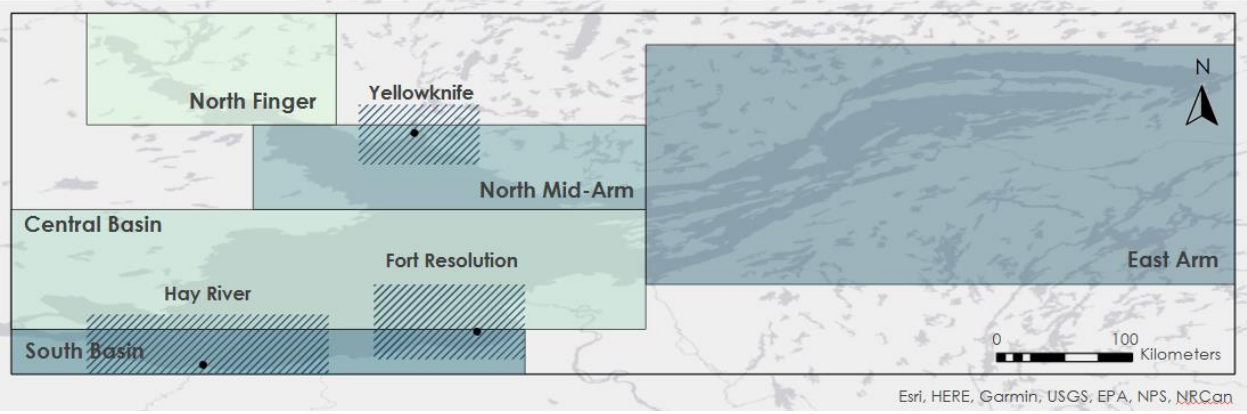

Figure 2. Study area map of Great Slave Lake, divided into five sections for further analysis. The boxes indicate the boundaries of each region, which were defined to assess spatial variations in turbidity.

2. Methodology

2.1 Data Acquisition

2.1.1 Satellite Data

When calculating turbidity from Earth observations, using imagery with relatively longer wavelength reflectance bands in a range from 400 nm to 900 nm provided the most precise results compared to in situ measurements (Dogliotti, et al. 2015). Therefore, to assess the turbidity for regional areas of the lake with a long timescale, we compared imagery from three different satellites and wavelengths. We accessed Aqua MODIS, Level 3, monthly average remote sensing reflectance (Rrs) data at the 678 nanometer (nm) wavelength from the Ocean Color Data website (Table 1) from 2002 to 2024. We accessed ESA's Ocean-Colour Climate Change Initiative (OC-CCI), 6.0 release, monthly average reflectance data at the 665 nm wavelength from 2002 to 2024 (Table 1). ESA's OC-CCI is a long-term consistent global ocean color dataset, produced by merging reflectance data from multiple satellite sensors, including NASA's Sea-viewing Wide Field-of-view Sensor, Aqua MODIS and Visible Infrared Imaging Radiometer Suite, as well as ESA's Medium Resolution Imaging Spectrometer (MERIS) and Sentinel-3 Ocean and Land Colour Instrument (OLCI) sensors. OC-CCI is helpful for aquatic ecosystem research because the dataset is pre-processed, reliable, and errors are quantified (Sathyendranath et al. 2019). Finally, we accessed the Sentinel-3A, Level 3, monthly average reflectance data at 709 nm from 2016 to 2024 downloaded from NASA's Ocean Color Web database within the Ocean Biology Distributed Active Archive Center (OB.DAAC) (Table 1). We completed a quality assurance check between the long-term MODIS imagery at 678 nm (Rrs678) and OC-CCI imagery at 665 nm (Rrs665), and the short-term Sentinel-3A imagery at 709 nm (Rrs709).

To analyze turbidity at a localized scale, specifically at Hay River, Fort Resolution, and Yellowknife, we used Sentinel-2 Multispectral Imager (MSI), Level-2A data at the 865nm wavelength band (Table 1). The Sentinel-2 MSI sensor has a spatial resolution of 20m. Our science advisor, Dr. Cédric Fichot, and his graduate student, Hangjie Lin, from the Aquatic Photo-biogeochemistry and Remote Sensing lab, provided the localized imagery, with an applied atmospheric correction, via a shared Google Drive folder. Fichot and Lin accessed the Landsat 8/9 and Sentinel-2 data from the NASA Earth Data and Copernicus Data Space Application Programming Interface (API) run in JupyterLab. The imagery underwent atmospheric correction through ACOLITE (Dark-Spectrum-Fitting approach), an open-source atmospheric correction program for aquatic environments run in Python.

Table 1. *Details from accessed remote sensing datasets*

Earth Observation Dataset	***Wavelength Band (nm)***	***Date Range***	***Data Source***	***Spatial Resolution (m)***	***Study Area Category***
Sentinel-3A OLCI	709	June – October 2016 – 2024	Ocean Data	4000	Regional
Aqua MODIS	678	June – October 2002 – 2024	Ocean Data	4000	Regional
Ocean Colour – Climate Change Initiative (OC-CCI)	665	June – October 2002 – 2024	OC-CCI	4000	Regional
Sentinel-2 MSI	704	June – October 2015 – 2024	Cédric Fichot	20	Localized

2.1.2. In situ Data

We acquired multiple in situ datasets, including surface reflectance and turbidity data collected by Dr. Cédric Fichot's team in Great Slave Lake during 2022-2024 and used it to create our reflectance to turbidity algorithms. For data validation we used Mackenzie Data Stream, a Canadian open-access hub for sharing water quality data, to access turbidity sampling data from the NWT-wide Community Based Water Quality Monitoring Program for four long-term monitoring sites in Great Slave Lake located near Hay River, Fort Resolution, and Yellowknife. Finally, to assess the impact of the Slave River discharge on Great Slave Lake's

turbidity, we obtained monthly mean discharge data from Environment and Climate Change Canada (ECCC) between 2002 and 2024 at the Fitzgerald, Alberta station — the closest Slave River hydrometric monitoring station to Great Slave Lake (Table 2) (Environment and Climate Change Canada, n.d.).

Table 2. *Details from accessed in situ datasets*

In situ Dataset	***Collection Method***	***Date Range***	***Source***	***Station***
River Discharge	Hydrometric Monitoring	2002 – 2024	Environment and Climate Change Canada	#07NB001, Fitzgerald, Alberta
Reflectance and Turbidity	YSI Sonde and Above Water Image Spectroscopy	2023 – 2024	Cédric Fichot	Vessel deployed sensors around GREAT SLAVE LAKE
Turbidity	YSI Sonde	2012 – 2023	Government of the Northwest Territories, NWT Community-based water quality monitoring program	Fort Resolution at Resolution Bay: RES-GREAT SLAVE LAKE Hay River at Mouth of Hay River: HAY-GREAT SLAVE LAKE Yellowknife at Great Slave Lake: YEL-GREAT SLAVE LAKE-Dettah YEL-GREAT SLAVE LAKE-N'Dilo

2.2 Data Processing

2.2.1 Turbidity Algorithms

Turbidity is a measure of the light scattered by suspended particles relative to that of a known standard (e.g., Formazin) and describes how clear or opaque water is (Mohammad et al., 2016). We used the in situ reflectance and turbidity data to determine a regression equation between these two variables to perform analysis on turbidity levels. In Excel 2016, we plotted turbidity versus reflectance at 665, 678, 709, and 704 nm (Figure 3). Then, for each wavelength, we generated regression equations using an exponential, power, second-order polynomial, and third-degree polynomial relationship. We determined the best regression equation for each wavelength by comparing the R^2 values, establishing the linear relationship between the predicted turbidity at each wavelength versus the in situ turbidity, and calculating the mean absolute percentage error. Determining which regression models provided the best fit for the in situ turbidity data through the R^2 value was important so that we could apply it to the various Earth observation reflectance imagery. We used these measures to collectively determine what regression equation to use as the "turbidity algorithm" for each wavelength (Table 3). The turbidity algorithm took a reflectance value for each pixel and converted it to a turbidity value through multiplication by coefficients (Table 3).

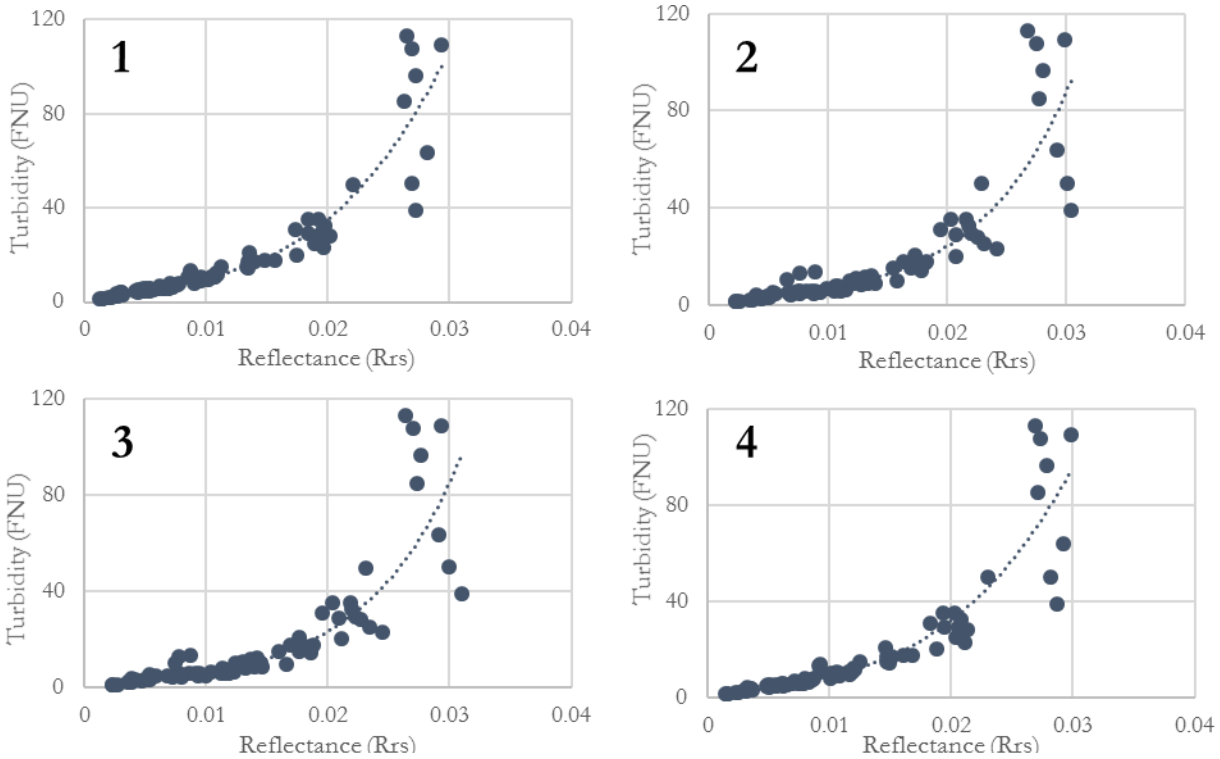

Figure 3. Scatterplots showing the regression relationship between in situ turbidity and reflectance we used to derive turbidity algorithms. The reflectance bands shown in these plots include: 1) 709nm 2) 678nm 3) 665nm 4) 704nm.

Table 3. *Details from Turbidity Algorithms*

Earth Observation Dataset	***Turbidity Algorithm Number***	***Turbidity (T) Algorithm***
Sentinel-3A OLCI	*1*	$T = 5{,}424{,}800.95 * (Rrs)^3 - 90{,}362.09 * (Rrs)^2 + 1{,}401.12 * (Rrs)$
Aqua MODIS	*2*	$T = 1.8653e^{128.32(Rrs)}$
Ocean Colour – Climate Change Initiative (OC-CCI)	*3*	$T = 1.7418e^{129.65(Rrs)}$
Sentinel-2 MSI	*4*	$T = 4{,}493{,}478.93\ (Rrs)^3 - 65{,}480.37(Rrs)^2 + 1{,}113.90(Rrs)$

2.2.2 Turbidity Imagery

We utilized our turbidity algorithms to transform all the downloaded reflectance imagery to turbidity imagery. In MATLAB 2017b, we cropped the Sentinel-3A and MODIS imagery to the extent of Great Slave Lake and then applied Turbidity Algorithm 1 and 2, respectively, from Table 3. We repeated this process for OC-CCI and also cropped the imagery to the localized sub-sections, North Finger, North Mid-Arm, Central Basin, South Basin, and East Arm, and used Turbidity Algorithm 3 from Table 3. For Sentinel-2 reflectance imagery,

we replicated the same process in MATLAB but cropped it to Hay River, Fort Resolution, and Yellowknife and applied Turbidity Algorithm 4 from Table 1.

2.2.3 In situ Data Comparison

In preparation for comparison with satellite-derived turbidity, we compiled turbidity data from the Mackenzie Data Stream collected from water sonde stations offshore of Hay River and Fort Resolution and two offshore of Yellowknife, within our localized analysis areas. To account for temporal mismatch, we paired the date of collection of our in situ turbidity data with our localized turbidity imagery (Sentinel-2). If a sonde recorded multiple measurements in a single day, we averaged those values when pairing it with a satellite image-derived value. We then calculated the average turbidity from the localized turbidity imagery using the pixel of the coordinates of the sonde and the eight adjacent pixels. Using R 4.4.2., we imported these averaged values into a merged dataset ready for analysis.

2.3 Data Analysis

2.3.1 Sensor Comparison

We produced a time series plot in R to compare the reflectance data between Sentinel-3, OC-CCI, and MODIS. We created this plot to validate the accuracy of using the 678 nm MODIS band and 665 nm OC-CCI band, which both have data from 2002 to 2024, instead of the 709 nm band in Sentinel-3, which only has data from 2016 to 2024. This comparison served as a quality assurance check between the shorter wavelength and longer-term MODIS and OC-CCI imagery versus the longer wavelength and shorter-term Sentinel-3 imagery.

2.3.2 Turbidity Time Series

Using R, we created time series scatterplots of remote sensing turbidity data derived from OC-CCI between 2002 and 2024. These plots helped us compare how the monthly average lake turbidity varied over time. We also created time series scatterplots of OC-CCI-derived remote sensing turbidity data for each subsection of the study area: North Finger, North Mid-Arm, Central Basin, South Basin, and East Arm. We compared the plots from each subsection to observe how turbidity patterns vary between different areas of the lake over time. We used R to generate OC-CCI data-derived turbidity imagery time-series maps for the full extent of Great Slave Lake as well as for each of the five regional sections. We compared these maps to each other to visualize turbidity patterns across the entire lake as well as in the different subsections. Turbidity maps for the three localized community areas, Hay River, Fort Resolution, and Yellowknife were created in R using Sentinel-2-derived data. We created these localized maps so that our partners could look at the turbidity data from 2015 to 2024 more visually compared to the previously provided plots. Due to the size of Great Slave Lake, localized maps are necessary to accurately analyze turbidity values at specific communities as requested by our partners. For the regional sections as well as Great Slave Lake, we created box plots of average remotely sensing turbidity values for each month from June to October across 22 years. We used these box plots to visualize how the turbidity values varied by month among different regional sub-sections of Great Slave Lake. This approach helped evaluate how turbidity changes month-to-month and provided information on the potential drivers of seasonal variability.

2.3.3 Turbidity Versus Average Discharge

For the entirety of Great Slave Lake and for each of the five regional sections, we created scatterplots of average monthly remotely sensed turbidity versus average monthly in situ river discharge data from the Slave River. We used these scatterplots to compare how the discharge from the Slave River into Great Slave Lake affected the turbidity levels in different sections of the Great Slave Lake.

2.3.4 In situ Validation

To determine how well our turbidity algorithms performed, we created scatterplots comparing the in situ turbidity data from the NWT-wide Community-based Monitoring Program to the Sentinel-2 reflectance turbidity. For each area, we used Excel to plot actual versus predicted turbidity values and applied a linear regression model to evaluate their relationship. Comparison between in situ and remotely sensed turbidity

values was important to test if our turbidity algorithms accurately predicted in situ turbidity values and whether they may confidently be used in the future to monitor turbidity in this region.

3. Results

3.1 Analysis of Results

3.1.1 Sensor Comparison Results

The turbidity measurements from Aqua MODIS using Rrs678 and OC-CCI using Rrs665 yielded similar monthly average turbidity measurements to those obtained with Sentinel-3A using Rrs709. Aqua MODIS and OC-CCI generally reported slightly higher turbidity values compared to Sentinel-3A (Figure 4). Aqua MODIS and OC-CCI showed moderately strong correlations with Sentinel-3A with R^2 values of 0.81 and 0.71, respectively (Figure A1). However, a few potential outliers above a turbidity of 9 Formazin Nephelometric Units (FNU) caused the observed regression lines to deviate away from the ideal regression line, suggesting that Aqua MODIS and OC-CCI may be less accurate at measuring higher turbidity values. The ideal regression line represents the scenario where Aqua MODIS and OC-CCI theoretically provide the same turbidity measurements as Sentinel-3A.

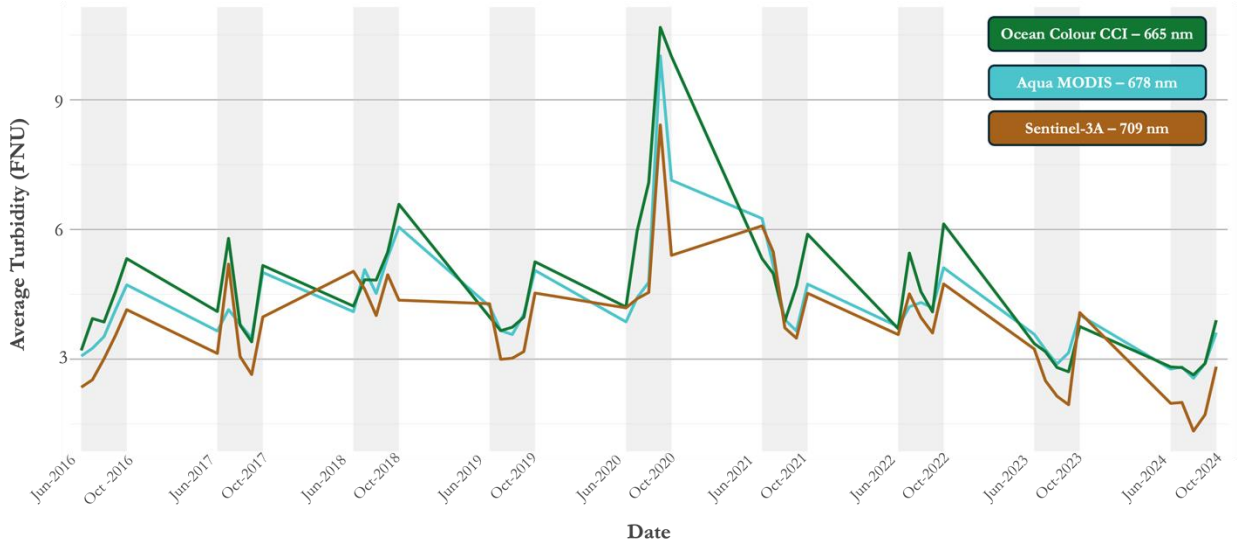

Figure 4. Monthly average turbidity measurements from Sentinel-3A, Aqua MODIS, and OC-CCI, June to October, 2016-2024.

3.1.2 Turbidity Timeseries Results

The average monthly turbidity of Great Slave Lake remained relatively consistent between 2002 and 2019, fluctuating between 4 and 6 FNU, with a slight dip from 2014 to 2016 (Figure 5). A sharp spike occurred in 2020, resulting in a record-high lake-wide turbidity, followed by a record-low lake-wide turbidity in 2024. Regionally, the North Finger had the highest monthly average turbidity peaking at approximately 100 FNU in September 2012. The East Arm had the lowest monthly average turbidity fluctuating around 1.8 to 2.2 FNU with a slight increase to around 2.6 FNU in 2011. The North Mid-Arm, Central Basin, and South Basin all had similar trends, mostly ranging from 2 to 10 FNU, and all three regions experienced a spike in 2020 (Figure 5).

Seasonally, turbidity gradually increased from June to October throughout the 22-year study period, with October having the highest monthly average turbidity across Great Slave Lake and all five regions. Throughout the study period, the North Finger, East Arm, and South Basin showed a steady rise from June to October, while the North Mid-Arm experienced a slight dip in July before increasing through October. In the Central Basin, turbidity was similar in July and October but showed fluctuations between these months (Figure 5).

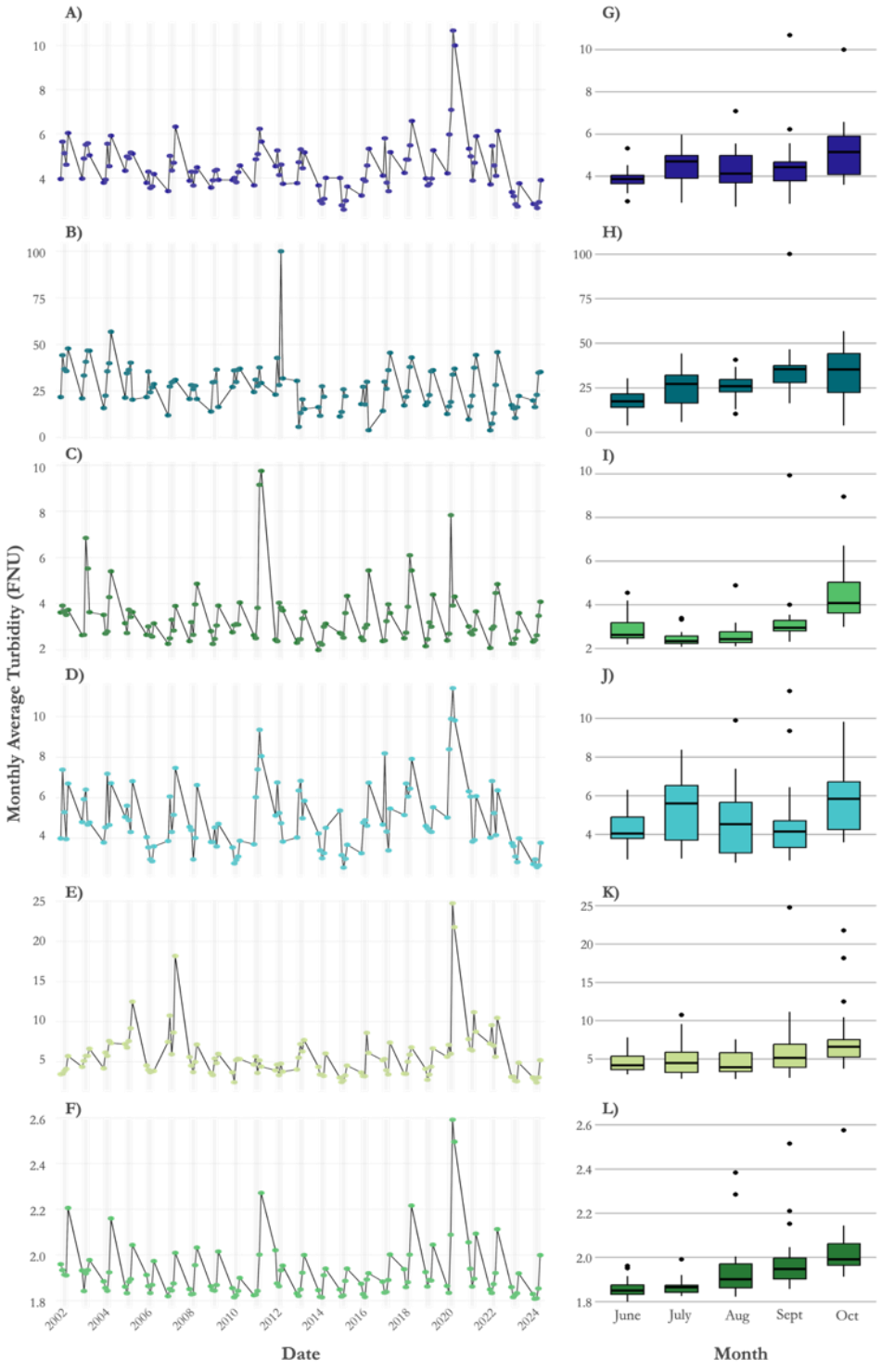

Figure 5. Time series (A–F) and seasonality boxplots (G–L) of monthly average turbidity across the entire Great Slave Lake and its five regions. Each time series plot (A–F) represents monthly average turbidity trends from 2002 to 2024, while the corresponding boxplots (G–L) display the seasonal distribution of turbidity within each region. The regions are labeled as follows: (A, G) entire lake, (B, H) North Finger, (C, I) North Mid-Arm, (D, J) Central Basin (E, K) South Basin, and (F, L) East Arm.

3.1.3 Slave River Discharge and Turbidity Results

Slave River discharge influenced GREAT SLAVE LAKE turbidity, but its impact varied across regions. Overall, the correlation was weak, with an R^2 value of 0.185 for all GREAT SLAVE LAKE. The Central Basin, which contains the Slave River's mouth, showed the strongest correlation ($R^2 = 0.276$), suggesting a localized influence on turbidity. The nearby South Basin also had a weak correlation ($R^2 = 0.126$). Moreover, the North Finger, North Mid-Arm, and East Arm showed little to no relationship, with R^2 values of 0.037, 0.007, and 0, respectively (Figure 6).

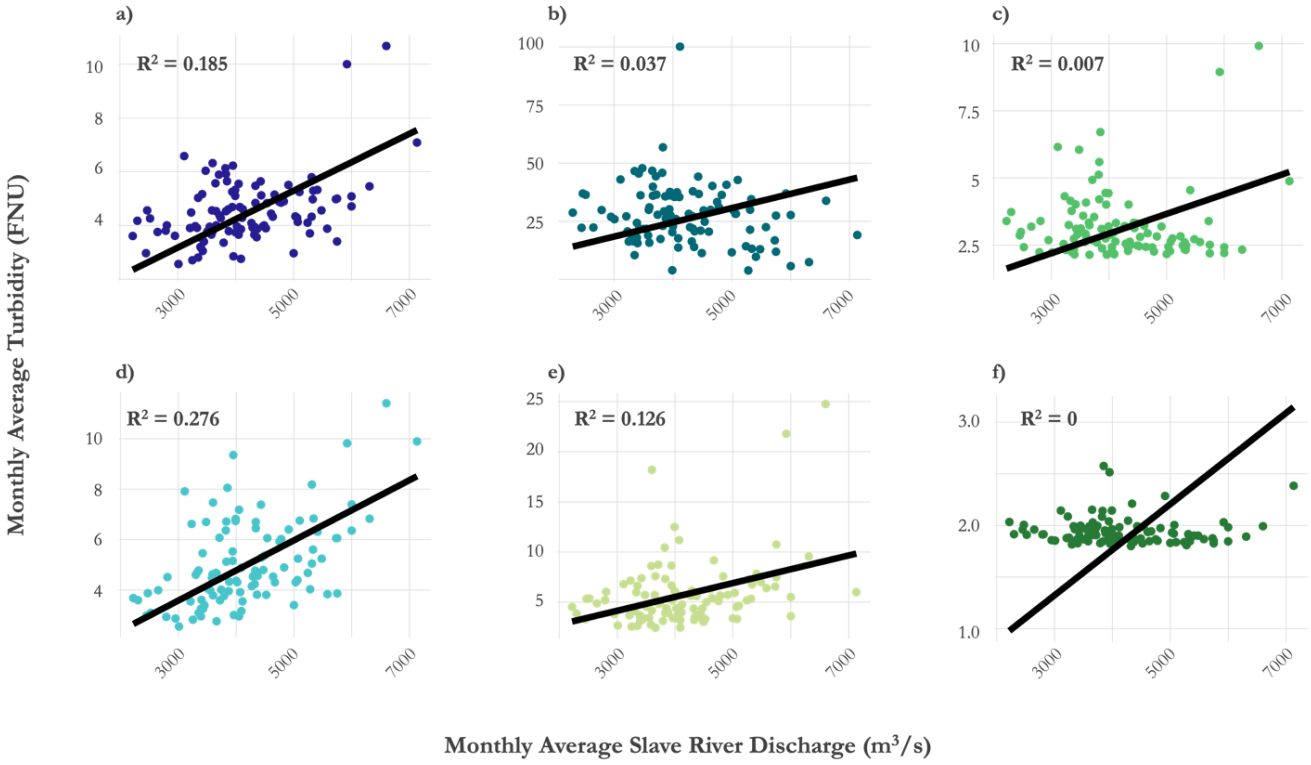

Figure 6. Scatterplots showing the relationship between monthly average turbidity and Slave River discharge across different regions of Great Slave Lake: a) entire lake b) North Finger, c) North Mid-Arm, d) Central Basin, e) South Basin, and f) East Arm.

3.1.4 In situ Validation

Comparison between the calculated turbidity from Sentinel-2 imagery and in situ data revealed that there was a slight predictive relationship for these sampling locations (Figure 7). The R^2 values derived from the regression analysis in Figure 7 indicated the strongest relationship within the Yellowknife localized region which included data from two long term sampling sites. Our algorithms for Sentinel-2 consistently overpredicted turbidity for Hay River and Fort Resolution and underpredicted turbidity for Yellowknife. However, both Hay River and Fort Resolution still showed fair to moderate evidence of a correlation.

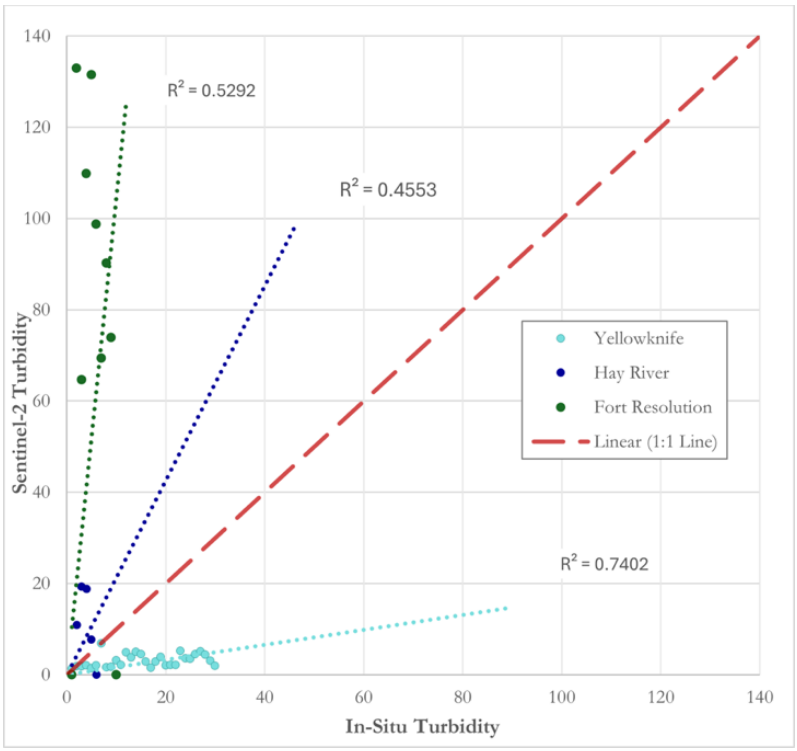

Figure 7. Scatterplot showing the relationship between turbidity derived from Sentinel-2 and in situ turbidity measurements from GNWT YSI sondes for the three localized areas

3.2 Errors & Uncertainties

Each data source used in this feasibility study had its own set of uncertainties and limitations. Our Earth observations were constrained by a combination of spectral and temporal resolution. Since moderate turbidity estimates are most accurately derived from Rrs in the near-infrared, we prioritized using Sentinel-3A, which offered the longest wavelength (709 nm) among our Earth observation sources and thus provided the best band for reflectance measurements. However, Sentinel-3 data were only available from 2016 onward, limiting its use for our 22-year study period. Consequently, we also used OC-CCI, which covered our study period from 2002 but operates at a shorter wavelength of 665nm.

We faced limitations with spatial resolution between the Earth observation sensors. OC-CCI has a relatively coarse resolution of 4km which allowed us to analyze averages over large areas and time periods but did not provide detailed information on smaller regions. Specifically, the East Arm of Great Slave Lake contains small lakes and islands that potentially affected remote sensing reflectance values, as the sensor could not distinguish between multiple features contained within the same pixel and therefore could not count a pixel with a combination of land and water as just land. Conversely, Sentinel-2 offered high spatial resolution, making it ideal for analyzing localized areas, though it was limited by low temporal resolution due to infrequent data collection by the satellite. Furthermore, seasonal ice coverage on Great Slave Lake obstructed both satellite and in situ data collection during the colder months, limiting our analysis to the period from June through October.

Variations in the number of viable pixels available to calculate monthly turbidity averages contributed to uncertainties in our data. In 2012, the number of pixels dropped significantly by approximately 3000 for the entire lake – across all regions due to the removal of the MERIS sensor from the OC-CCI dataset (Figure 8). The North Finger consistently had the fewest pixels throughout the 22-year study period due to its small size, OC-CCI's low spatial resolution, and varying ice cover in October. The low pixel counts for the North

Finger, which ranged from zero to around 300, likely contributed to the region recording the highest turbidity averages compared to other sections of the lake as they may be affected more by outliers.

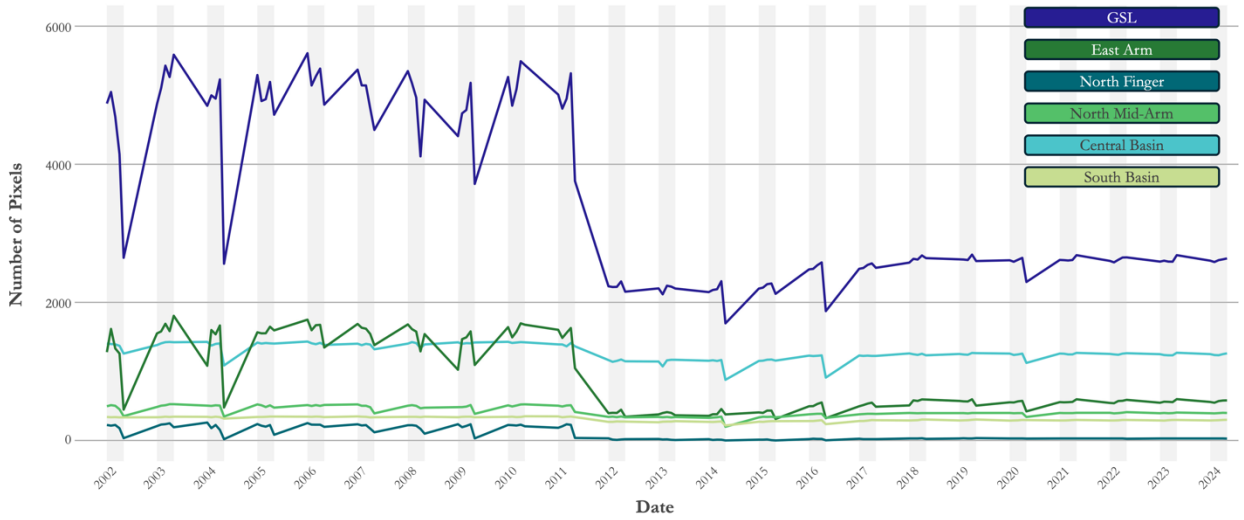

Figure 8. Time series of number of pixels used to calculate each OC-CCI monthly average turbidity image in Great Slave Lake and its 5 regions.

Our in situ turbidity and reflectance data (Fichot, 2022-2024) were limited by the size of the lake, its terrain, and available resources. This limited dataset did not fully represent turbidity across the entire lake and affected the accuracy of our turbidity algorithms. Furthermore, the YSI Sonde data from the GNWT contained limited temporal matches with Sentinel-2 observation dates, and while the sonde collected measurements within a 24-hour period, there were inconsistencies in the number and timing of observations available. A 3-hour window would have provided a more accurate comparison with Sentinel-2 data by addressing the hourly variations commonly seen in turbidity.

4. Conclusions

4.1 Interpretation of Results

Our findings demonstrated that implementing Earth observations is a feasible method for monitoring turbidity in Great Slave Lake. By applying remotely sensed turbidity values, we analyzed water resources across different spatial and temporal scales, revealing both the strengths and limitations of this approach for lake-wide water quality monitoring. Identifying and utilizing suitable Earth observation sensors for turbidity monitoring allowed us to develop and validate algorithms to accurately measure turbidity over 22 years. Specifically, our results revealed that shorter wavelength imagery from OC-CCI is a reliable tool for predicting turbidity levels, providing a solid foundation for future long-term monitoring efforts. Our findings also suggest that Sentinel-2 imagery may be used at the localized scale to assess turbidity, although more detailed and temporally consistent in situ datasets are needed to further validate the strength of its predictive power. Additionally, the weaker relationship between in situ and satellite-derived turbidity at Hay River and Fort Resolution, compared to Yellowknife – which generally experiences lower turbidity – suggests that these algorithms may be more accurate in areas with lower turbidity.

While our remote sensing methods effectively tracked turbidity trends, our results did not reveal a strong correlation between turbidity and Slave River discharge. However, the study did highlight the presence of regional fluctuations in turbidity levels across the lake, emphasizing the dynamic nature of water quality in response to a range of environmental factors. These fluctuations suggest that while Slave River discharge may not necessarily be a primary driver of turbidity, other localized factors such as wind-driven suspension and seasonal algal blooms may play a significant role in influencing turbidity. This conclusion underscores the

feasibility of using remote sensing techniques to monitor turbidity at finer spatial scales, offering precise insights into how turbidity varies across such a large and complex system as Great Slave Lake.

4.2 Feasibility & Partner Implementation

Our Earth observations results complement in situ data, allowing our partners to use remote sensing techniques for effective turbidity monitoring at both local scales and across large regions, such as the entirety of Great Slave Lake. Our study found that satellite-derived turbidity data provides valuable large-scale spatial and temporal insights that can complement the routine site-specific water quality sampling conducted on Great Slave Lake by GNWT. This approach expands data collection to remote and hard-to-access areas, offering a more comprehensive understanding of turbidity dynamics. By leveraging Earth observations, our partner's lake-wide accessibility, funding, and temporal limitations can be sufficiently addressed. Additionally, the turbidity visualizations we created will help communities and stakeholders better understand the spatial patterns of turbidity at various timestamps, which is essential for making informed decisions regarding water quality management, conservation efforts, and the protection of fisheries across various locations on Great Slave Lake. Ultimately, the integration of Earth observation tools into monitoring practices can empower local communities to preserve their natural resources and respond proactively to changes in water quality. As remote sensing technology continuously improves, this satellite data will become more reliable in providing stand-alone products for use in Great Slave Lake.

5. Acknowledgements

Science Advisors:

- Dr. Cedric Fichot (Boston University)
- Hanjie Lin (Boston University)

Partners:

- Guylaine Ross (Government of the Northwest Territories)
- Robin Staples (Government of the Northwest Territories)
- Jennifer Hickman (Government of the Northwest Territories)

Collaborators:

- Mike Tollis (Akaitcho Territory Government)
- Claudia Azigwe (K'atl'odeeche First Nation)

Lead:

- Madison Arndt (DEVELOP MA – Boston)

Project Coordination Point of Contact

- Isabel Tate (DEVELOP Project Coordination Fellow)

This material contains modified Copernicus Sentinel data (2016 - 2024), processed by ESA.

Any opinions, findings, and conclusions or recommendations expressed in this material are those of the author(s) and do not necessarily reflect the views of the National Aeronautics and Space Administration.

This material is based upon work supported by NASA through contract 80LARC23FA024.

6. Glossary

ACOLITE - A generic processor for atmospheric correction and processing for coastal and inland water applications
Algal Bloom – A rapid increase in the density of algae in an aquatic system, often caused by nutrient pollution
Chl-a - Chlorophyll-A

Discharge - A volume of water flowing through a specific cross-sectional area of a stream or river per unit of time
Drainage Basin – An area of land drained by a river and its tributaries, forming a natural watershed
Earth observations - Satellites and sensors that collect information about the Earth's physical, chemical, and biological systems over space and time
FNU – Formazin Nephelometric Units
Frequency Band - A range or interval of electromagnetic frequencies used to transmit signals
Hydrometric - The monitoring and measurement of the components of the hydrological cycle, including rainfall, groundwater, and surface water flow and quality
In situ - Refers to local, on-site or in-position observation data collected from ground, sea, or air-borne sensors
Mean Absolute Percentage Error - A measure of prediction accuracy of a forecasting method in statistics, calculated by dividing the absolute difference between the actual and predicted values by the actual value, multiplying by 100 and then averaging all the percentage errors
MODIS – Moderate Resolution Imaging Spectroradiometer
NIR - Near-Infrared Spectroscopy
OC-CCI – Ocean Colour Climate Change Initiative
OLCI - Ocean and Land Color Instrument
Polynomial - An equation formed with variables, exponents, and coefficients, where the exponents are non-negative integers, set equal to zero
R^2 Value - A measure that provides information about the goodness of fit of a model
Reflectance - The ratio of the amount of light reflected by a surface to the amount of light incident on that surface
Regression Equation - A statistical technique that relates a dependent variable to one or more independent variables
Remote Sensing - Techniques and processes for detecting the physical qualities of an area by measuring the radiation reflected and emitted by that area from a distance, usually from satellites or aircraft
Rrs - Remote Sensing Reflectance
Seasonality - The quality of an environmental pattern of change to occur along a predictable time scale
Sediment - The conglomerate of materials, organic and inorganic, that can be carried away by water, wind or ice
Spatial Resolution - The smallest size of an area for which a given sensor can distinguish that area from its surroundings. Spatial resolution for imagery is often reported in terms of pixel size, or the geographic distance covered by the length of one image pixel
Temporal Resolution - The unit of time between observations in a dataset of repeated measurements. This may also be referred to as the return frequency or observation frequency
Time Series - A sequence of data points indexed or listed in time order, commonly used to analyze trends, patterns, and relationships over time, and can be used for forecasting
Turbidity - A hydrological metric that describes how clear or opaque water using the amount of light scattering
YSI Sonde - Multiparameter water quality sensors produced by Yellow Springs Instruments

7. References

Communities of the Northwest Territories; NWT-wide Community Based Water Quality Monitoring Program; Government of the Northwest Territories, Environment and Climate Change. 2024. *NWT-wide Community-based Monitoring Program* (Version 10.1.0.) [Data set]. DataStream. https://doi.org/10.25976/4der-gd31

Dogliotti, A., I., Ruddick, K. G., Nechad, B., Doxaran, D., & Knaeps, E. (2015). A single algorithm to retrieve turbidity from remotely-sensed data in all coastal and estuarine waters. *Remote Sensing of Environment*, 156, 157-168. https://doi.org/10.1016/j.rse.2014.09.020

Environment and Climate Change Canada (n.d.). *Historical Hydrometric Data: Slave River at Fitzgerald (Alberta)*. [Data set]. Environment and Climate Change Canada. Retrieved from: https://wateroffice.ec.gc.ca/report/historical_e.html?stn=07NB001

European Space Agency (ESA). (2021). *Copernicus Sentinel-2 MSI Level-2A Reflectance Product (Collection 1)* [Data set]. European Space Agency. Retrieved June 2024. https://doi.org/10.5270/S2_-znk9xsj

Earth Resources Observation and Science (EROS) Center. (2020). Landsat 8-9 Operational Land Imager Sensor Level-2, Collection 2 [Data set]. U.S. Geological Survey. https://doi.org/10.5066/P9OGBGM6.

Evans, M. S., & Muir, D. C. G. (2016). Persistent organic contaminants in sediments and biota of Great Slave Lake, Canada: Slave River and long-range atmospheric source influences. *Journal of Great Lakes Research*, 42(2), 233–247. https://doi.org/10.1016/j.jglr.2015.12.001

Fichot, C. (2022-2024) [YSI Sonde and above water image spectroscopy of Great Slave Lake using vessel deployed sensors] [Unpublished raw data]. Boston University.

Gibson, J. J., Prowse, T. D., & Peters, D. L. (2006). Hydroclimatic controls on water balance and water level variability in Great Slave Lake. *Hydrological Processes*, 20(19), 4155–4172. https://doi.org/10.1002/hyp.6424

Government of the Northwest Territories. (n.d.). *Wide community-based water quality program.* NWT Water Stewardship. https://www.nwtwaterstewardship.ca/en/nwt-wide-community-based-water-quality-program

Mohammad, H. G., Melesse, A. M., & Reddi, L. (2016). A Comprehensive Review on Water Quality Parameters Estimation Using Remote Sensing Techniques. *Sensors*, 16(8), 1298. https://doi.org/10.3390/s16081298

NASA Goddard Space Flight Center, Ocean Ecology Laboratory, Ocean Biology Processing Group. (2022). *Moderate-resolution Imaging Spectroradiometer (MODIS) Aqua Level-3 Mapped Remote-Sensing Reflectance* (Version 2022) [Data set]. NASA OB.DAAC. Retrieved March 13, 2025, from https://doi.org/10.5067/AQUA/MODIS/L3M/RRS/2022

NASA Goddard Space Flight Center, Ocean Ecology Laboratory, Ocean Biology Processing Group. (2022). *Ocean and Land Colour Imager (OLCI) SENTINEL-3A Level-3 Mapped Earth Observation Reduced Resolution Remote-Sensing Reflectance* (Version 2022) [Data set]. NASA OB.DAAC. Retrieved March 13, 2025, from https://doi.org/10.5067/SENTINEL-3A/OLCI/L3M/ERR/RRS/2022

Pearson, R. W. (1970). *Resource Management Strategies And Regional Viability: A Study Of The Great Slave Lake Region, Canada* (Publication No. 7021034). [Doctoral dissertation, University of Illinois at Urbana-Champaign]. ProQuest Dissertations Publishing.

Pour, H. K. (2011). *On the Use of MODIS for Lake and Land Surface Temperature Investigations in the Regions of Great Bear Lake and Great Slave Lake, N.W.T.* [Unpublished master's thesis]. University of Waterloo. https://uwspace.uwaterloo.ca/items/334331fe-dea3-4022-8cd3-c3abf634155c

Sathyendranath, S., Brewin, R. J. W., Brockmann, C., Brotas, V., Calton, B., Chuprin, A., Cipollini, P., Couto, A. B., Dingle, J., Doerffer, R., Donlon, C., Dowell, M., Farman, A., Grant, M., Groom, S., Horseman, A., Jackson, T., Krasemann, H., Lavender, S., Martinez-Vicente, V., Mazeran, C., Mélin, F., Moore, T. S., Müller, D., Regner, P., Roy, S., Steele, C. J., Steinmetz, F., Swinton, J., Taberner, M., Thompson, A., Valente, A., Zühlke, M., Brando, V. E., Feng, H., Feldman, G., Franz, B. A., Frouin, R., Gould, R. W., Hooker, S. B., Kahru, M., Kratzer, S., Mitchell, B. G., Muller-Karger, F. E., Sosik, H. M., Voss, K. J., Werdell, J., & Platt, T. (2019). An ocean-colour time series for use in climate studies: The experience of the Ocean-Colour Climate Change Initiative (OC-CCI). *Sensors*, 19(19), 4285. https://doi.org/10.3390/s19194285

Sathyendranath, S.; Jackson, T.; Brockmann, C.; Brotas, V.; Calton, B.; Chuprin, A.; Clements, O.; Cipollini, P.; Danne, O.; Dingle, J.; Donlon, C.; Grant, M.; Groom, S.; Krasemann, H.; Lavender, S.; Mazeran, C.; Mélin, F.; Müller, D.; Steinmetz, F.; Valente, A.; Zühlke, M.; Feldman, G.; Franz, B.; Frouin, R.; Werdell, J.; Platt, T. (2023): *ESA Ocean Colour Climate Change Initiative (Ocean_Colour_cci): Monthly climatology of global ocean colour data products at 4km resolution, Version 6.0. NERC EDS Centre for Environmental DataAnalysis*. (Version 6.0.) [Data set]. CEDA Archive. https://catalogue.ceda.ac.uk/uuid/690fdf8f229c4d04a2aa68de67beb733/.

Rühland, K. M., Evans, M., & Smol, J. P. (2023). Arctic warming drives striking twenty-first century ecosystem shifts in Great Slave Lake (Subarctic Canada), North America's Deepest Lake. *Proceedings of the Royal Society B: Biological Sciences*, 290(2007), Article 13. https://doi.org/10.1098/rspb.2023.1252

Appendix A

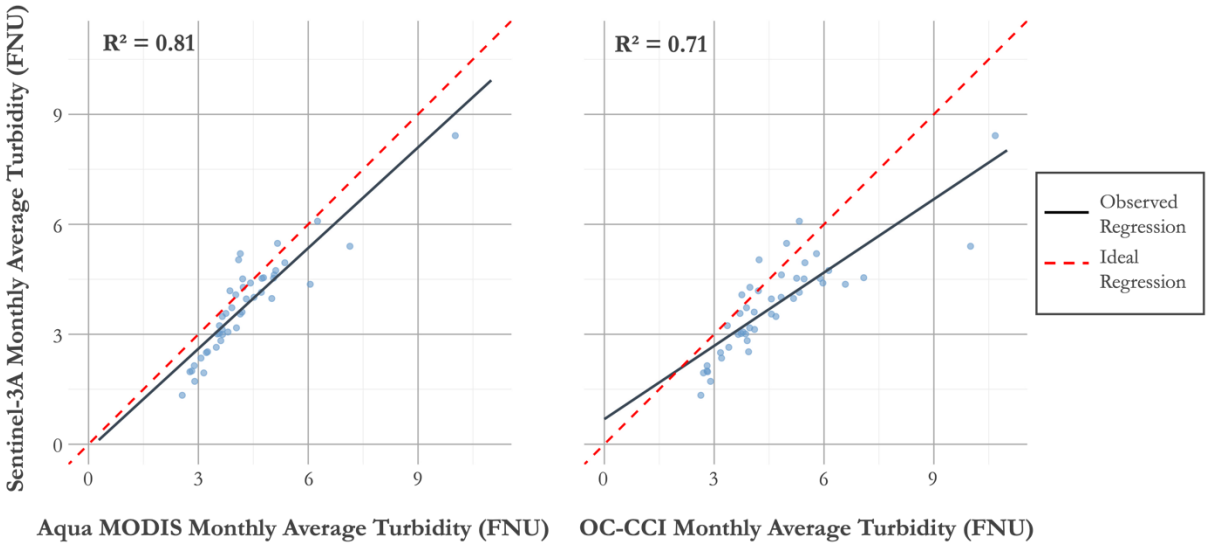

Figure A1. Scatterplots comparing monthly average turbidity measurements between Sentinel-3A and Aqua MODIS (left) and Sentinel-3A and OC-CCI (right).